NASA TECHNICAL NOTE

NASA TN D-7760

ANALYSIS OF A FLARE-DIRECTOR CONCEPT FOR AN EXTERNALLY BLOWN FLAP STOL AIRCRAFT

by David B. Middleton

Langley Research Center
Hampton, Va. 23665

1. Report No. NASA TN D-7760	2. Government Accession No.	3. Recipient's Catalog No.
4. Title and Subtitle ANALYSIS OF A FLARE-DIRECTOR CONCEPT FOR AN EXTERNALLY BLOWN FLAP STOL AIRCRAFT		5. Report Date November 1974
		6. Performing Organization Code
7. Author(s) David B. Middleton		8. Performing Organization Report No. L-9572
9. Performing Organization Name and Address NASA Langley Research Center Hampton, Va. 23665		10. Work Unit No. 504-29-14-01
		11. Contract or Grant No.
12. Sponsoring Agency Name and Address National Aeronautics and Space Administration Washington, D.C. 20546		13. Type of Report and Period Covered Technical Note
		14. Sponsoring Agency Code

15. Supplementary Notes

16. Abstract

A flare-director concept involving a "thrust-required" flare-guidance equation has been developed and demonstrated during tests on a moving-base simulator. The equation gives a signal to command thrust as a linear function of the errors between the variables thrust, altitude, and altitude rate and corresponding values on a desired reference flare trajectory. During the simulator landing tests this signal drove either the horizontal command bar of the aircraft's flight director or a thrust-command dot on a "head-up" virtual-image display of a flare director. It was also used as the input to a simple auto-flare system.

An externally blown flap STOL (short take-off and landing) aircraft (with considerable stability and control augmentation) was modeled for the landing tests. The pilots considered the flare director a valuable guide for executing a proper flare-thrust program under instrument-landing conditions, but were reluctant to make any use of the head-up display when they were performing the landings visually.

17. Key Words (Suggested by Author(s)) Flare-director STOL aircraft Externally blown flaps Thrust flare	18. Distribution Statement Unclassified — Unlimited STAR Category 02		
19. Security Classif. (of this report) Unclassified	20. Security Classif. (of this page) Unclassified	21. No. of Pages 23	22. Price* $3.00

ANALYSIS OF A FLARE-DIRECTOR CONCEPT FOR AN EXTERNALLY BLOWN FLAP STOL AIRCRAFT

By David B. Middleton
Langley Research Center

SUMMARY

A study has been made of the use of a "thrust-command" flare director for more precise control of an externally blown flap (EBF) STOL aircraft during short-field landings. A flare-director equation composed of both "reference" and measured variables was developed and demonstrated on a moving-base simulator. This equation gave a signal to command thrust as a linear function of the errors between the variables thrust, altitude, and altitude rate and corresponding values on a desired reference flare trajectory. The signal was displayed on the simulated aircraft's regular flight director for instrument-flight-rules (IFR) landings and on a "head-up," virtual-image flare director for visual-flight-rules (VFR) landings. (The virtual-image display was superimposed on the landing scene and focused at infinity.) This signal was also used as the input to an autoflare system.

Fifty simulated landing approaches were made at 75 knots along a 6° glide slope to a specified altitude where a constant-attitude power flare was initiated by the pilot. Moderate turbulence was present during some runs. The following findings were among those obtained during the simulation:

(1) Under IFR conditions the flare-director information, presented on the horizontal command bar of the flight director, was judged a valuable guide in executing a proper thrust program for the flare.

(2) Under VFR conditions, the virtual-image presentation of the flare director was rated undesirable by the pilots because they felt the need to fixate on the runway instead of the director as the aircraft approached touchdown. (Not enough time was available for them to switch their attention back and forth.) However, the pilots demonstrated that they could make good landings if they forced themselves to concentrate on the virtual-image flare director and to monitor the visual scene in their peripheral vision, but they said that they would not like to land a real airplane in this manner.

INTRODUCTION

Precise control of short-take-off-and-landing (STOL) aircraft during landing approach is generally more difficult than it is for conventional-take-off-and-landing (CTOL) aircraft of similar size. Steeper glide slopes and smaller landing zones are used by the STOL aircraft, and thus the flare is of relatively short duration. STOL aircraft handling qualities (at the low landing speeds) are generally poor, and system lags become increasingly more significant as the glide slope is steepened. For STOL aircraft equipped with externally blown flaps, the control problem is further complicated by the so-called "negative ground effects" (lift losses as the aircraft nears the ground plane). Thus, there would appear to be little margin for piloting error during a final approach and flare initiation, and very little possibility of correcting large "off-nominal" conditions once the flare was underway. To be assured of passenger acceptance, however, STOL landings should be no less comfortable or safe than present airline landings with CTOL aircraft.

In several recent fixed-base simulation studies (refs. 1 to 3) of landing approaches with a medium-range STOL aircraft equipped with externally blown flaps, the handling qualities of the aircraft were rated poor, and consistent control of the touchdown conditions was a problem. This problem was alleviated somewhat by the addition of several types of stability and control augmentation to the aircraft. Further improvement was achieved by using a 2-segment glide slope $\left(\text{e.g., } 7\frac{1}{2}^{\text{O}} \text{ initial and } 4^{\text{O}} \text{ final}\right)$; however, such a profile would require more elaborate ground equipment at each airport. Even with these improvements, there was still a large variation in the flare profiles and subsequent touchdown conditions. The primary causes were identified as (1) the brevity of the flare maneuver, (2) system lags, and (3) the lack of easy-to-follow flare-guidance information. Real-world landings with a STOL aircraft equipped with externally blown flaps under VFR conditions are expected to be better than simulated ones because better visual and motion cues are inherently available. However, for poor visibility conditions, an improvement of the guidance information seemed the next logical step needed to produce consistently good flares; therefore, the present study was undertaken.

One approach to providing better information is to have a thrust-command signal composed of time-dependent elements as well as measured ones. A signal of this type is developed herein. During a series of simulated landing approaches, this signal was presented to the pilot (1) on the horizontal command bar of the flight director and (2) on a head-up virtual-image display superimposed on the simulated landing scene. The simulation results are included in this report. Prior to the piloted runs the signal was also fed into a simple autoflare system and tuned to reproduce (approximately) the calculated reference flare trajectory.

SYMBOLS

In order to facilitate international usage of the data presented, dimensional quantities are presented both in the International System of Units and in U.S. Customary Units. Dots over symbols denote differentiation with respect to time.

C_D drag coefficient

C_L lift coefficient

$\Delta C_{L,ge}$ incremental lift coefficient due to ground effect

C_{L_α} lift coefficient due to changes in angle of attack

C_m pitching-moment coefficient

C_μ thrust coefficient

ΔC_μ incremental thrust coefficient

g acceleration due to gravity, meters/second^2 (feet/second^2)

h altitude, meters (feet)

h_{cg} vertical distance from aircraft center of gravity to landing gear, meters (feet)

h_f altitude of center of gravity at flare initiation, meters (feet)

h_R reference altitude during calculated flare trajectory, meters (feet)

I_X, I_Y, I_Z moments of inertia about aircraft body axes

I_{XZ} product of inertia

K_i constant coefficients in equation (1) (i = 1,2,3,4)

T thrust, newtons (pounds force)

ΔT_c incremental thrust command during flare (see eq. (1)), newtons (pounds force)

T_R reference thrust during calculated flare trajectory, newtons (pounds force)

t_f time duration of flare, seconds

t_l time left until touchdown, seconds

V_A aircraft velocity (airspeed), meters/second (feet/second)

V_h horizontal component of V_A, meters/second (feet/second)

V_i inertial velocity of aircraft, meters/second (feet/second)

X distance from runway threshold, positive down runway, meters (feet)

X_f approximate flare range beyond glide-slope intercept with runway, meters (feet)

α angle of attack, degrees

γ flight-path angle, degrees

γ_f flight-path angle at flare initiation, degrees

θ_f constant pitch angle during flare, degrees

Abbreviations:

CTOL   conventional take-off and landing

EBF   externally blown flap

IFR   instrument flight rules

RDS   Real-Time Dynamic Simulator

STOL   short take-off and landing

VFR   visual flight rules

GENERAL CONSIDERATIONS

The powered-lift flaring technique considered herein consists generally of an initial step increase in throttle, followed by a steady advance until touchdown. It was developed during the study conducted in reference 1 of the EBF-STOL aircraft depicted in figure 1. Details of a typical wing section for this type of aircraft are shown in figure 2. The aerodynamic characteristics were determined from the wind-tunnel data curves of references 4, 5, and 6, and the engine characteristics were obtained from the manufacturer. Both sets of characteristics are tabulated in reference 1. Automatic speed control (autospeed) and "pitch hold" were among the augmentation systems recommended (ref. 1) for this aircraft, and both were used in the present study. Such features allow the landing attitude (pitch angle) to be established prior to initiation of the flare maneuver. Lateral-directional augmentation was also included in the simulation, but it had little effect on the results of the study.

Flare-Director Signal

Even though the basic flaring technique was the same as that used in the study reported in reference 1, the pilots in the present study had somewhat different flare-guidance information. In particular, a dominant "reference thrust" component based on the aerodynamic and exhaust-flow characteristics of the EBF-STOL aircraft was included in the thrust-command flaring signal. This signal, composed of both time-dependent reference variables and measured ones, has the following mathematical form:

$$\Delta T_c = K_1 \left[K_2 \left(T_R - T \right) + K_3 \left(h_R - h \right) + K_4 \left(\dot{h}_R - \dot{h} \right) \right] \tag{1}$$

where T, h, and $\dot{h}$ are the measured thrust, altitude, and altitude rate, respectively; the subscript R indicates reference variable; and the K's are constant gains. (Values of the K's are given in the section "Simulation and Results.") The reference values were derived from the wind-tunnel data of references 4 and 6. Reference flare trajectories were constructed in the form of thrust, altitude, and altitude-rate time histories. These reference curves were then combined with corresponding measured variables to form the difference expressions shown in equation (1). It was assumed that thrust could be measured or determined with sufficient accuracy for use in the present concept.

In the formulation of the flare-director signal, no consideration was given to such things as variations in landing weight and ambient temperatures. However, moderate turbulence was included in a number of test runs during the simulation, and the altitude and altitude-rate terms in the flare equation acted as correctors for off-nominal conditions.

Weight, N (lbf)   245 096 (55 100)

Wing area, m^2 (ft^2)   78 (843)

Wing span, m (ft)   24 (78)

Mean aerodynamic chord, $\bar{c}$, m (ft)   3.58 (11.74)

Center-of-gravity location, percent $\bar{c}$ 40

I_X, kg-m^2 (slug-ft^2)   331 103 (244 212)

I_Y, kg-m^2 (slug-ft^2)   334 637 (246 819)

I_Z, kg-m^2 (slug-ft^2)   625 677 (461 482)

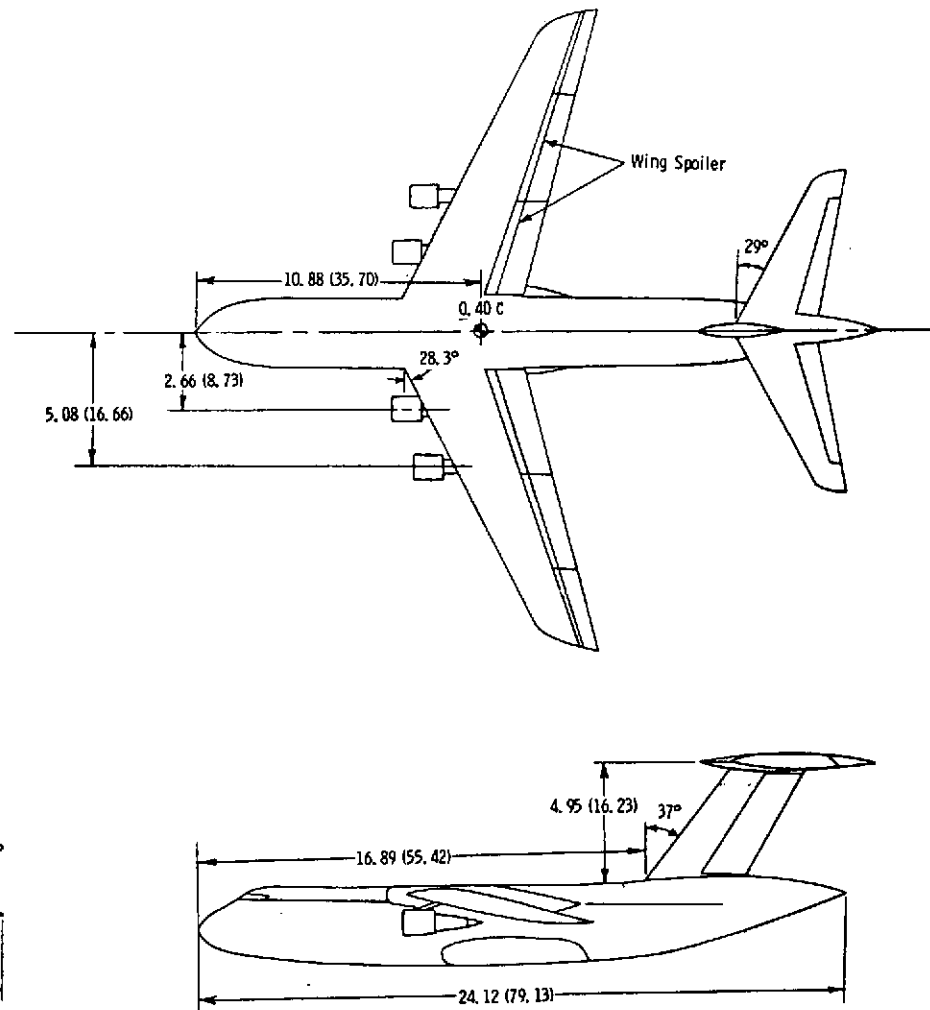I_{XZ}, kg-m^2 (slug-ft^2)   27 690 (20 423)

Figure 1.- Three-view drawing of simulated airplane.   All linear dimensions are in meters   (feet).
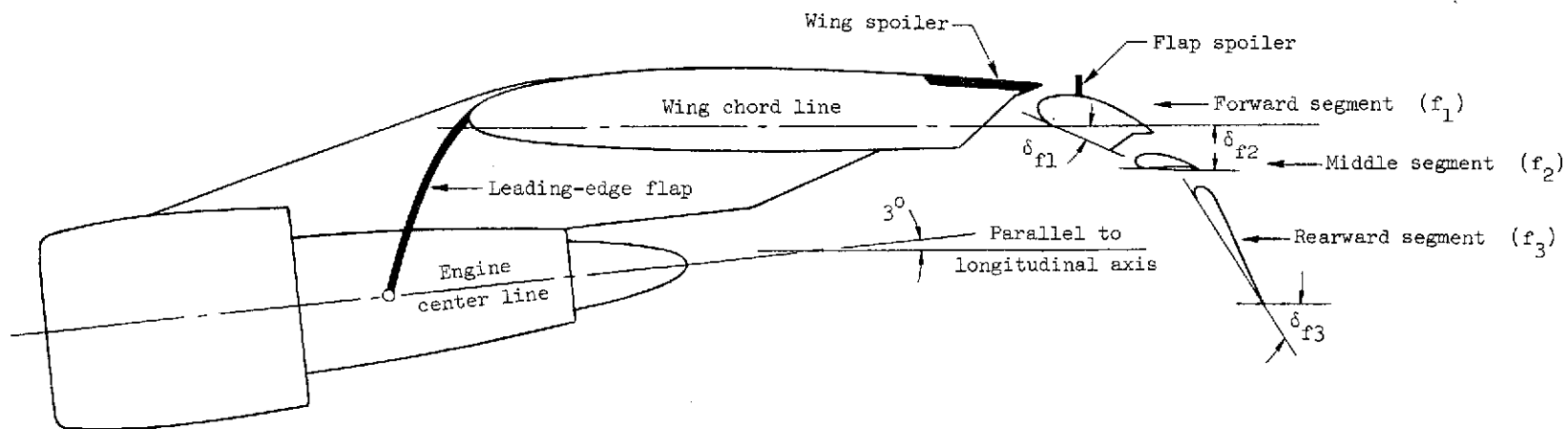
Figure 2.- Flap assembly and engine pylon detail. $\delta_{f1}/\delta_{f2}/\delta_{f3} = 25°/10°/60°$.

Reference Flare Trajectories

The reference flare trajectories developed in the following sections are the terminal segments of 75-knot landing approaches along a 6° glide slope. Such approaches imply a constant rate of sink ($\dot{h}$) of approximately 4 m/sec (13.23 ft/sec) along the glide slope prior to the flare. For purposes of this study, only one speed, weight, and landing trajectory were considered. The flare is initiated by changing $\ddot{h}$ (vertical acceleration) from 0 to some constant positive level and then maintaining this level until touchdown. The $\ddot{h}$ level is manipulated primarily by varying thrust, beginning with the step throttle increase at flare initiation and followed by a continuous increase until touchdown. The continuous increase is required (1) because the aircraft angle of attack α decreases with the flight-path angle γ during the flare and (2) because EBF aircraft experience lift losses near touchdown caused by negative "ground effects." (See the "Analysis" section of this paper.)

The altitude of flare initiation is selected so that $\dot{h}$ will be approximately 0 at touchdown. A second constraint requires that touchdown occur not more than 137 m (450 ft) beyond where the glide slope intersects the runway (at 76.2 m (250 ft) from the threshold). A further consideration in the selection of the flare altitude is to allow as much time as practical to execute the flare maneuver.

ANALYSIS

The flare task can be considered equivalent to changing the lift coefficient C_L of the aircraft from its steady-state value along the glide slope to an appropriately higher constant value for the flare. A thrust step at flare initiation is used to produce the new C_L value, and continuously increasing the thrust thereafter maintains this new value.

For the specified EBF-STOL aircraft and the selected landing-approach speed of 75 knots, the C_L was 3.43. This value was changed to $1 + (\ddot{h}/g)$ times 3.43 for the flare. Four levels of $\ddot{h}/g$ were considered initially in the data analysis that follows. These levels are listed in table I along with the constant C_L value associated with each. The other entries of table I are calculated in the following section.

Computations

The following equations are used to obtain h_f (flare-initiation altitude), t_f (duration of flare maneuver), and X_f (approximate flare range beyond glide-slope intercept with runway):

$$h_f = \left(\dot{h}_f^2 \middle/ 2\ddot{h} \right) + h_{cg}$$

$$t_f = \frac{\dot{h}_f}{\ddot{h}}$$

$$X_f = \left[V_i \cos\left(\frac{\gamma_f}{2}\right) \right] t_f - \left(h_f - h_{cg} \right) \cot \gamma_f$$

where $\dot{h}_f$ is the vertical velocity at flare initiation, h_{cg} is the distance from the air-craft center of gravity to its landing gear, and $V_i \cos\left(\frac{\gamma_f}{2}\right)$ is the average horizontal velocity during the flare. (The flight-path angle γ_f at flare initiation is assumed to be equal to the 6° glide-slope angle.) Values of t_f, h_f, and X_f for each of the four selected $\ddot{h}/g$ levels are shown in table I.

TABLE I.- VALUES OF FLARE-RELATED PARAMETERS FOR FOUR CONSTANT

LEVELS OF VERTICAL DECELERATION

$\ddot{h}/g$	C_L	t_f, seconds	h_f		X_f	
			meters	feet	meters	feet
0.05	3.60	8.22	20.22	66.35	159.10	521.99
.06	3.64	6.85	17.48	57.34	132.45	434.55
.07	3.67	5.88	15.51	50.90	113.76	373.78
.08	3.70	5.13	14.00	45.92	99.30	325.80

By applying the criterion $X_f < 137$ m (i.e., touchdown occurs within the specified landing zone (see ref. 1)), the deceleration-level choice $\ddot{h} = 0.05g$ is eliminated, and $\ddot{h} = 0.06g$ is marginal because even a slight delay in applying power would result in a touchdown beyond the landing zone. Then, on the basis that it would provide a longer flaring time, the choice was reduced to $\ddot{h} = 0.07g$.

Time Histories

Time histories of altitude h and altitude rate $\dot{h}$ were calculated from

$$h = \frac{1}{2} \ddot{h} t_l{}^2$$

$$\dot{h} = \ddot{h} t_l$$

where t_l is the time left until touchdown. These time histories are shown in figure 3. A time history of angle of attack α (as a function of t_l) is determined from

$$\alpha = \theta_f + \tan^{-1}\left(\frac{\dot{h}}{V_h}\right)$$

where θ_f is the pitch angle (assumed constant throughout the flare) and V_h is the horizontal velocity of the aircraft. The reference time history of α is also shown in figure 3. Because θ_f and V_h are approximately constant and $\dot{h}$ is a linear function of time, α also changes approximately as a linear function of time over a range of 2° to 8°. The α time history having been obtained, the curves of references 4 and 6 could then be used to construct a thrust time history for the selected $\ddot{h} = 0.07g$ level. For example, figure 29(c) of reference 4 contains wind-tunnel data curves for C_L, C_D, and C_m as a function of α for three constant thrust levels. Of these, C_L was by
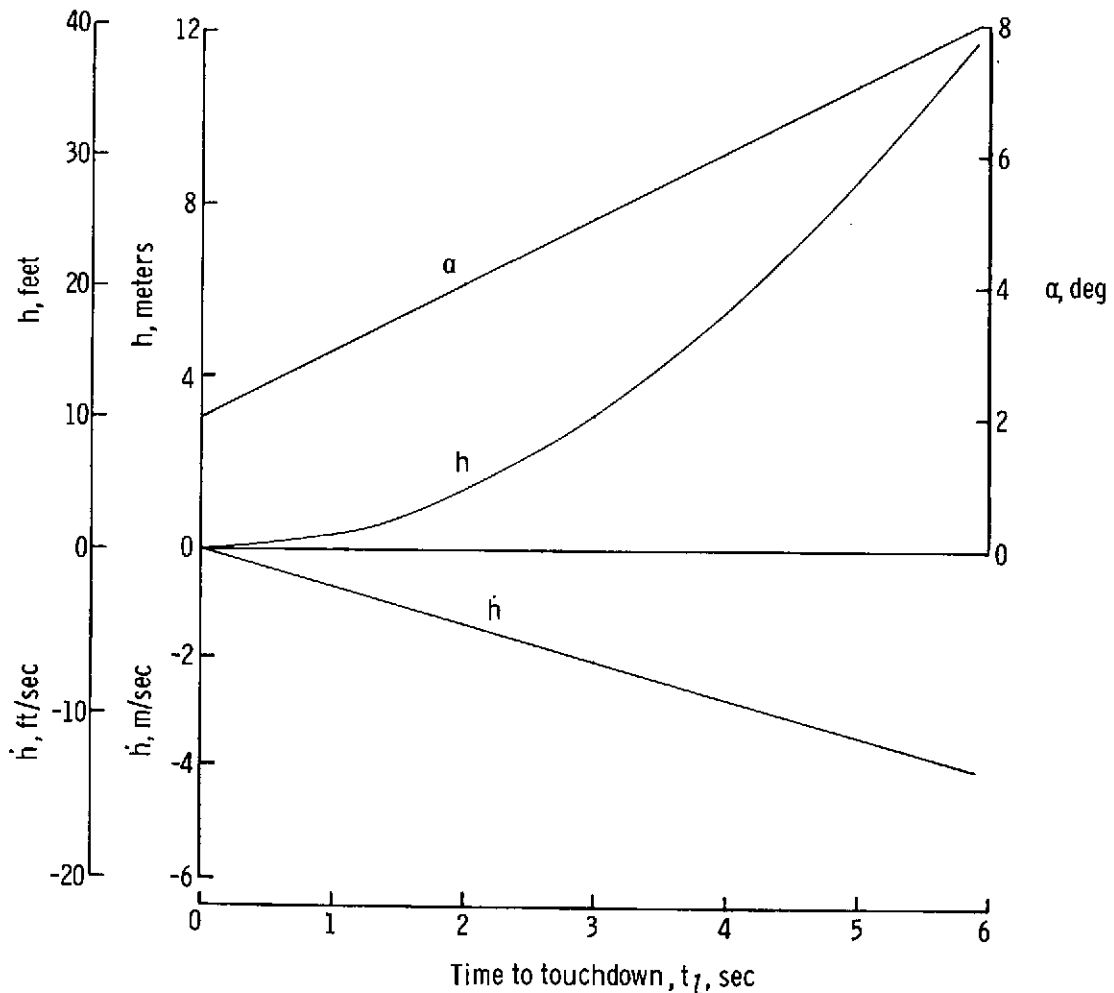

Figure 3.- Time histories of altitude h, altitude rate $\dot{h}$, and angle of attack α for the computed reference flare trajectory.

far the most sensitive to thrust change, particularly in the range of thrust and angle of attack considered. (In addition, changes in C_D caused by thrust change were negated by the autospeed feature, and the C_m data were also irrelevant because of the "pitch hold" augmentation system.)
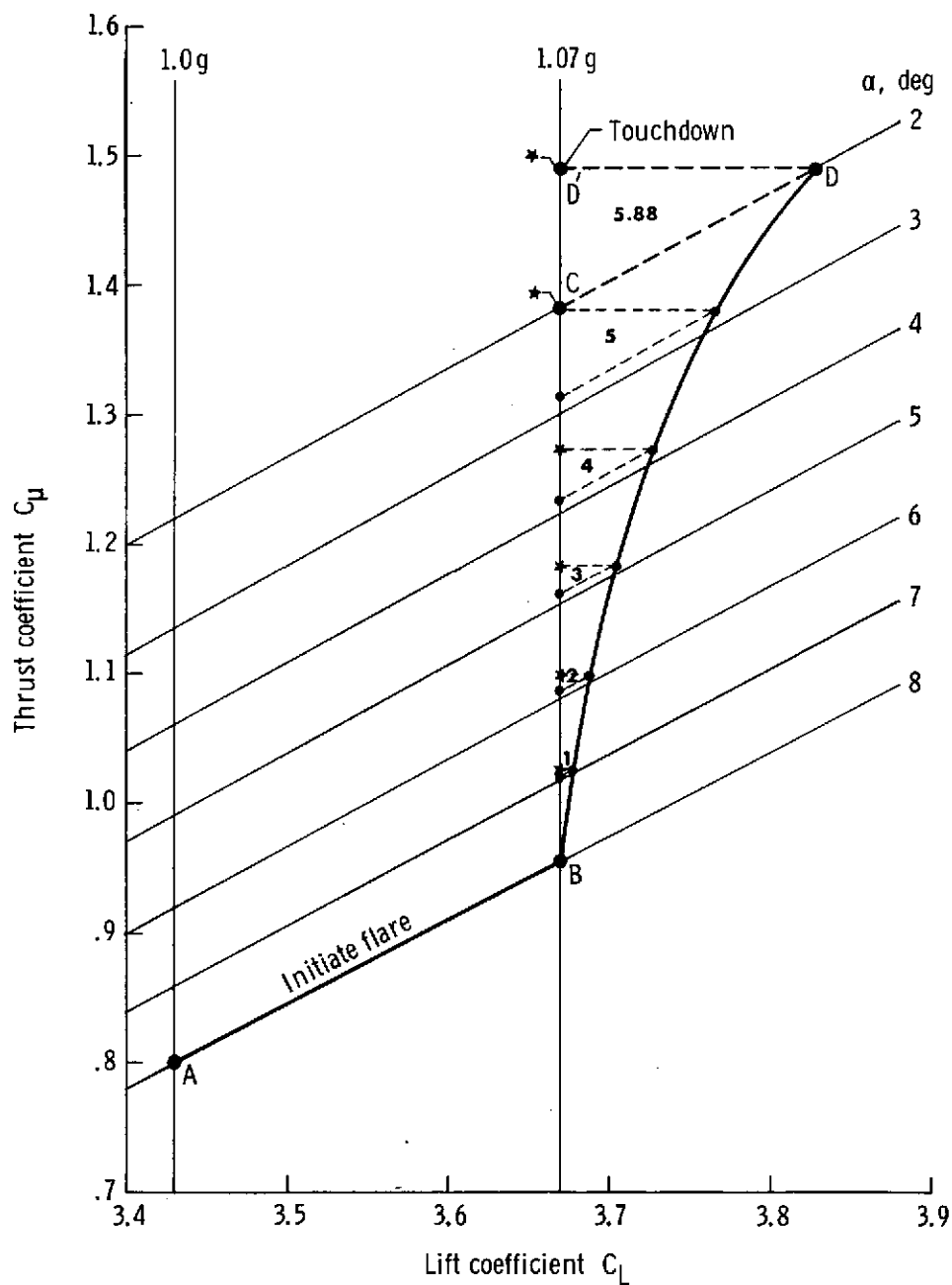

Figure 4.- Increase in thrust coefficient required for flare maneuver. (Stars identify total increase for each stated time.)

Figure 4 is a crossplot of a portion of the C_L data as a function of C_μ (thrust coefficient) for six increments in α. Vertical lines are used to identify (1) the $C_L = 3.43$ value for steady-state descent along the glide slope (labeled 1.0g) and (2) the $C_L = 3.67$ value used for the 0.07g flare maneuver (labeled 1.07g).

The nondimensional thrust increment ΔC_μ required for flare initiation can be determined directly from figure 4. For example, if $\theta_f = 2^O$ has been selected as the landing attitude, the intersection of the 1.0g vertical line with the $\alpha = 8^O$ curve (point A) yields $C_\mu = 0.80$ as the steady-state value while descending along the glide slope. Similarly, the intersection of the 1.07g vertical line with the same $\alpha = 8^O$ curve (point B) yields $C_\mu = 0.96$; hence, $\Delta C_\mu = 0.16$ is required for flare initiation. For the reference EBF-STOL aircraft this corresponds to approximately 11 120 N (2000 lbf) of thrust. For the engines used, this change was achieved in approximately 1 sec.

The requirement of additional C_μ to maintain the C_L flare value arises from two sources: (1) lift loss caused by the decreasing angle of attack $\left(\text{that is, } C_{L_\alpha} \text{ effect}\right)$ and (2) lift loss caused by the negative ground effects $\left(\text{expressed as } \Delta C_{L,ge}\right)$. The ΔC_μ required to compensate for the C_{L_α} effect $\left(\text{for } \theta_f = 2^O\right)$ is indicated by the line segment from point B to point C, and the additional C_μ required to compensate for the ground effects is represented by the segment from C to D'. Thus, a total $\Delta C_\mu \approx 0.53$ is required to maintain $C_L = 3.67$ during the flare.

The C_μ increase required to compensate for the C_{L_α} effect can be read directly along BC as a function of decreasing α. Then, using the α curve of figure 3, "time dots" are located along BC and identified each second (from B to C) by the numerals inside the dashed triangles. (These numerals also identify common times for the "time dots" along curve BD and "time stars" along BD'.)

The C_μ increase required to compensate for the $\Delta C_{L,ge}$ effects is derived from the "ground effects" data of reference 6. The $\Delta C_{L,ge}$ losses are first plotted as a function of altitude and then converted to an appropriate time history by use of the h curve of figure 3. In turn, the time history is converted into the BD curve of figure 4 with the aid of the α curve of figure 3. The horizontal dashed lines between the "time dots" on BD and the "time stars" on BD' represent the (predicted) $\Delta C_{L,ge}$ cumulative losses at each specified time interval. The solid-line side (vertical) of each triangle then represents the additional C_μ required to preclude the $\Delta C_{L,ge}$ losses during that interval, and the time stars identify the total C_μ required to maintain $C_L = 3.67$ at each interval during the flare. (It is coincidence that the time star for 5 sec falls almost directly on point C.)
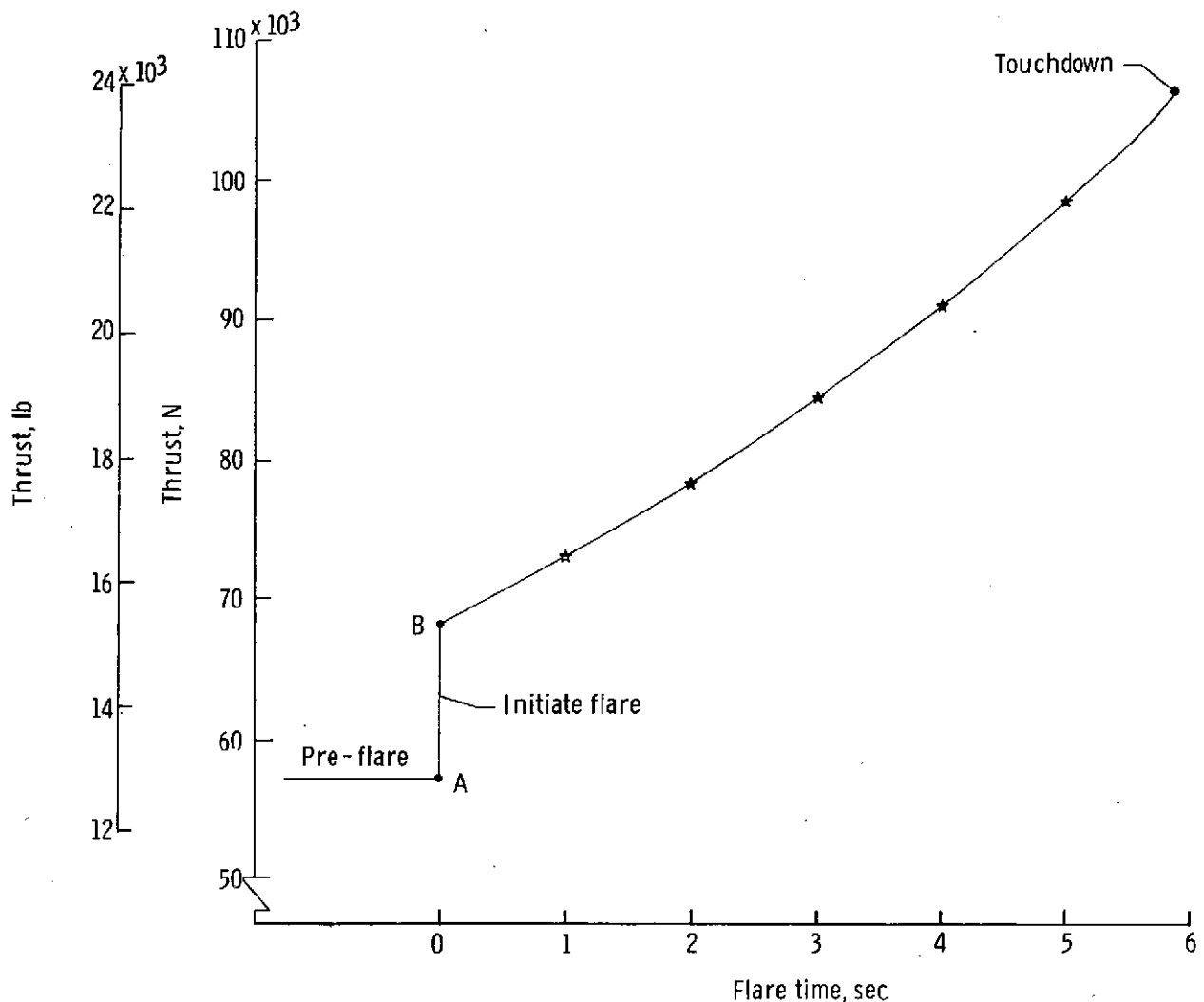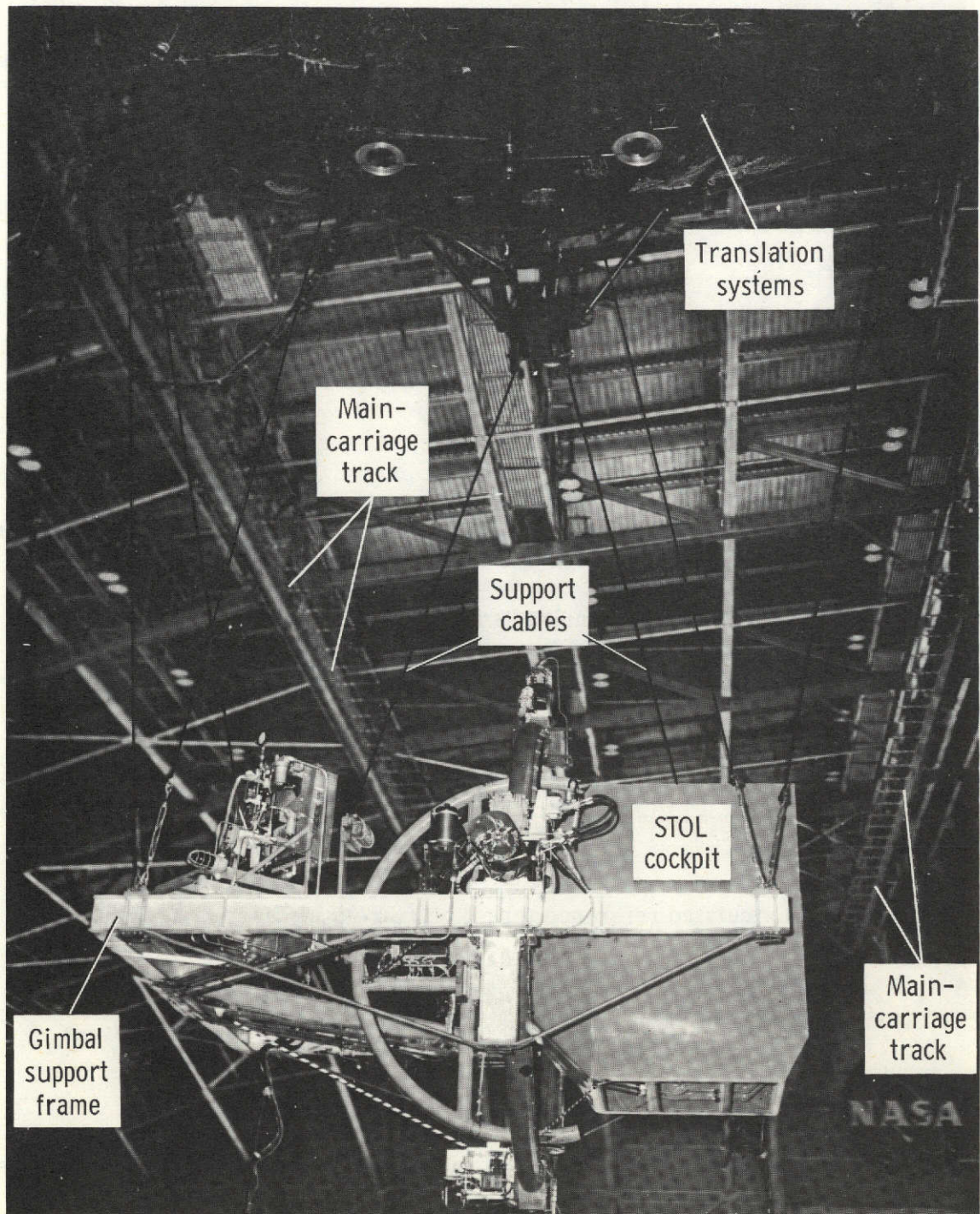
Figure 5.- Calculated reference thrust profile during flare maneuver.

A time history of thrust (converted C_μ values at the time stars) is shown in figure 5. This curve is then the basis of the T_R values used in equation (1).

SIMULATION AND RESULTS

To test the usefulness of the flare-director information developed herein, three sets of simulated landing-flare maneuvers were made on the Langley Real-Time Dynamic Simulator (RDS). The RDS is a six-degrees-of-freedom motion base simulator (see fig. 6) with an optional head-up virtual-image display of the landing terrain (shown in fig. 7).

Translation systems

Main-carriage track

Support cables

STOL cockpit

Gimbal support frame

Main-carriage track

NASA

L-74-1149

Figure 6.- Real-Time Dynamic Simulator (RDS) with cockpit of STOL aircraft mounted in the gimbals.
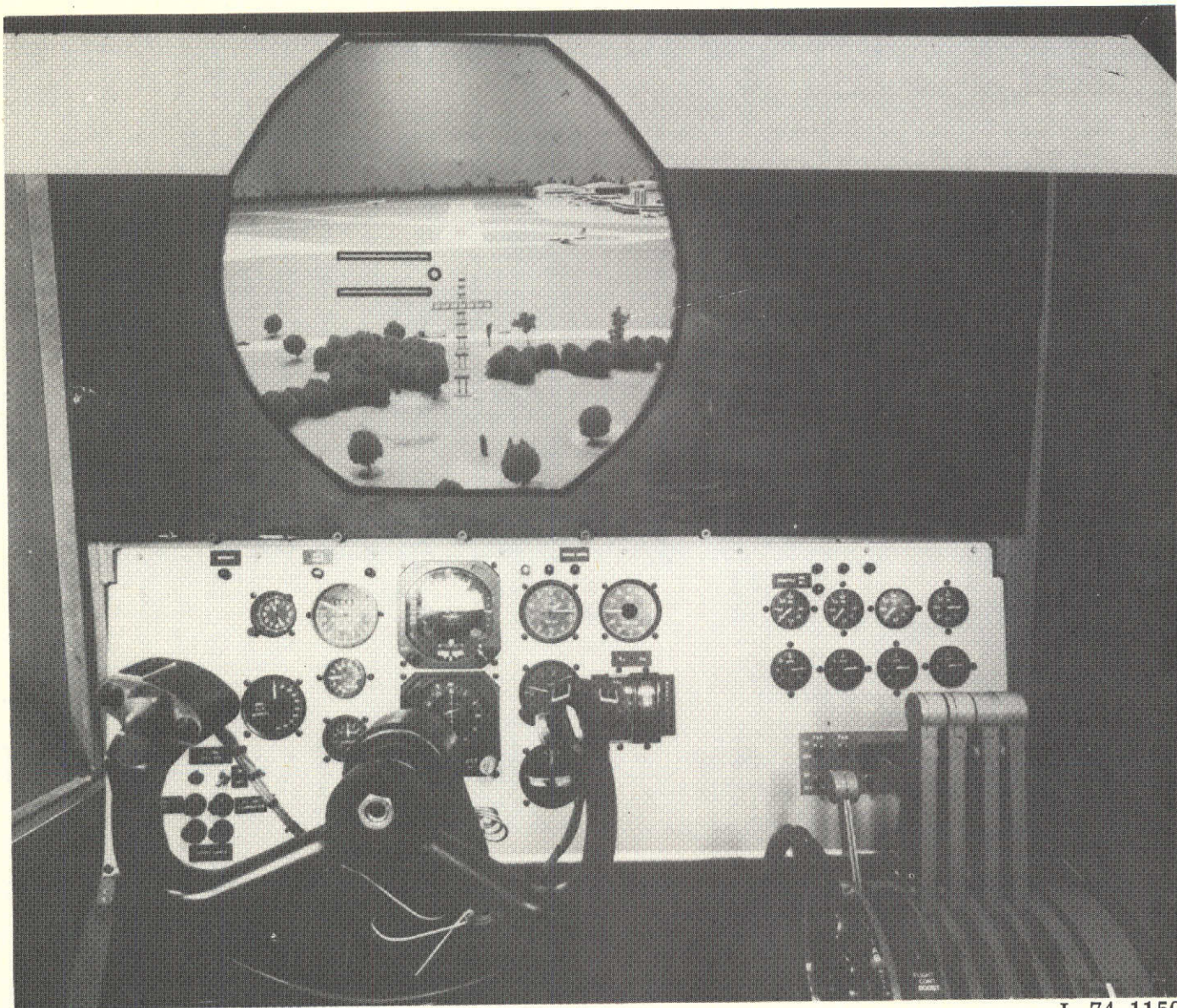
L-74-1150

Figure 7.- Pilot's view of inside of cockpit of STOL aircraft equipped for VFR approaches.

TABLE II.- RESULTS OF STOL LANDINGS WITH TWO FLARE-DIRECTOR CONFIGURATIONS

UNDER A VARIETY OF SIMULATED CONDITIONS

Run group	No. of runs	Conditions[a]	Location of flare director	Flare-light lead time, sec	Touchdown values[b]						Success index[c]
					Thrust		X, from threshold		Vertical velocity		
					newtons	lbf	meters	feet	m/sec	ft/sec	
A-1	7	Autoflare	Autoflare	0.0	101 188 (845)	22 748 (190)	130.17 (5.72)	427.08 (18.76)	0.88 (0.20)	2.90 (0.64)	1.000
A-2	5	Autoflare	Autoflare	0.4	102 900 (1913)	23 133 (430)	147.57 (6.19)	484.16 (20.32)	0.57 (0.12)	1.86 (0.41)	1.000
A-3[d]	4	Autoflare	Autoflare	0.6	104 835 (89)	23 568 (20)	149.59 (7.79)	490.79 (25.55)	0.43 (0.03)	1.42 (0.11)	0.500
B-1	3	M	None	--	108 483 (5155)	24 388 (1159)	203.95 (8.15)	669.14 (267.43)	1.18 (0.08)	3.88 (0.25)	0.667
B-2	2	M-T	None	--	97 727 (9928)	21 970 (2232)	140.22 (9.99)	460.03 (32.77)	2.13 (0.54)	6.98 (1.76)	0.000
B-3	12	M	On flight director	0.4	92 051 (7860)	20 694 (1767)	168.17 (43.61)	551.75 (143.10)	1.02 (0.37)	3.34 (1.23)	0.750
B-4	6	M-T	On flight director	0.4	97 264 (2015)	21 866 (453)	141.36 (29.19)	463.79 (95.77)	1.13 (0.43)	3.70 (1.42)	1.000
C-1	6	M-V	None	--	91 419 (6743)	20 552 (1516)	190.52 (102.72)	625.07 (337.02)	0.98 (0.66)	3.23 (2.16)	0.500
C-2	11	M-V	None	0.4	82 736 (18 278)	18 600 (4109)	177.03 (93.92)	580.82 (308.15)	1.40 (0.96)	4.58 (3.14)	0.364
C-3	8	M-V	Out window	0.4	94 671 (6316)	21 283 (1420)	127.17 (28.73)	417.21 (94.27)	1.37 (0.33)	4.51 (1.07)	0.625
C-4	2	M-T-V	Out window	0.4	86 664 (9577)	19 483 (2153)	207.23 (66.45)	679.90 (218.02)	0.74 (0.20)	2.42 (0.65)	0.500

[a]Letters have the following meanings: M, simulator motion; T, moderate turbulence; V, visual scene out window.

[b]Top number of each pair is the mean and (number) below it is standard deviation.

[c]Ratio of touchdowns within zone with $\dot{h} < 1.5$ m/sec (5 ft/sec) to number of runs.

[d]Two of the four runs in group A-3 ended in overflares; data averaged for two good runs.

The results of the landing-flare maneuvers are given in table II. The three sets of runs (A-, B-, C-) are in turn broken down according to the simulated flight conditions, which included the various combinations of motion, turbulence, visual scene, flare-warning light, and flare director. The location of the flare director (head up or on the flight director) was an additional parameter. Only a few runs were made in each category because they were conducted on a time-available basis during the study conducted in reference 3. The final column in table II ("Success index") gives the ratio of touchdowns within the designated landing zone with $\dot{h} \leq 1.5$ m/sec (5 ft/sec) to the total number of runs for that subset. The designated landing area for the simulated EBF-STOL aircraft was 76 m $\leq$ X $\leq$ 213 m (250 ft $\leq$ X $\leq$ 700 ft). The pilots were not given the option of a go-around, and this had some effect on the large dispersion in X values at touchdown.

The first set of runs (A-) was made with automatic thrust control during the flare to verify that equation (1) would produce a usable flare-director signal. The pilot tracked the glide slope down to the selected flare-initiation altitude and pushed a button to activate the automatic flare. The signal gains (i.e., values of the coefficients in eq. (1)) were adjusted during the A-1 runs to obtain a working set of values with respect to run-to-run variations in the aircraft state variables at flare initiation. The selected values were

$$K_1 = 0.0001$$

$$K_2 = 1.0$$

$$K_3 = 100$$

$$K_4 = -400$$

They produced a mean vertical velocity $\dot{h}$ at touchdown of approximately 0.9 m/sec (2.9 ft/sec). Subsets A-2 and A-3 were made with the same K values, but a flare warning light prompted the pilot to push the autoflare button a fraction of a second before the designated flare-initiation altitude was reached. The lead time of 0.4 sec in the A-2 runs produced an $\dot{h}$ of less than 0.6 m/sec (2 ft/sec) at touchdown. A lead time of 0.6 sec (A-3 runs) produced an even lower $\dot{h}$ value, but there were overflares in 2 runs. Rather than "retuning" the autoflare system, these K values and the 0.4-sec lead time were accepted as good working numbers for the piloted runs which followed.

Prior to the data flights, the pilots each made several practice runs in both smooth air and moderate turbulence. They indicated that for the turbulence runs they desired a smoother command signal — one that was less responsive to $\dot{h}$ errors. At the end of the practice session they agreed on the following set of K values (used in all set B- and C- runs):

$$K_1 = 0.00015$$

$$K_2 = 1.0$$

$$K_3 = 200$$

$$K_4 = 0$$

The rationale for this selection was that in turbulence the $\left(\dot{h}_R - \dot{h}\right)$ term caused annoying fluctuations in the command signal which had to be averaged out mentally; thus, by setting

17

$K_4 = 0$, the $\left(T_R - T\right)$ term dominated to produce the smooth, easy-to-follow signal the pilots sought. Compromise values of $K_4 = -200$ and $K_4 = -100$ were tested but not preferred to $K_4 = 0$. The gain K_3 was, however, doubled to increase the weight of the altitude errors, and the overall gain K_1 was increased.

The second set of runs (B-) was made under instrument-flight-rules (IFR) conditions with motion and moderate turbulence (where indicated). No flare director or warning light was used in baseline subsets B-1 and B-2. In subsets B-3 and B-4 the flare-director signal was automatically switched into the thrust command-channel (horizontal bar) of the flight director when the aircraft reached the designated flare-initiation altitude. The pilot observed this switchover as a sudden upward jump in the command bar, due to the $\left(T_R - T\right)$ term in eq. (1), and he took immediate action to drive the bar back to center by applying more thrust T. The flight director is shown in figure 8, and it appears as number 7 in the simulator instrument array pictured in figure 9. (The flare warning light is number 9 in this array.) As indicated earlier, this light allowed the pilot to anticipate the flare and quickly move (or be moving) the throttles when the command bar jumped.

As expected, the pilots expressed a definite preference for flaring with the flare director and commented that they knew intuitively when to start increasing the thrust; without the command bar, however, they had no positive guide as to how much or how fast to continue the increase. The data (table II), although sparse, support their contention that their landings were somewhat better when the flare director was used (compare subsets B-1 and B-3) and much better when it was used in turbulence (compare subsets B-2 and B-4).

The third set of runs (C-) was made with visual flight rules (VFR) with several display variations. A closed-circuit television and virtual-image lens system were used to televise and display an out-the-window view of a STOL airport (see fig. 7). A second television camera was focused on an abstract flare-director display consisting of one or two fixed horizontal reference lines and a moving dot driven by the "equation (1)" signal. When two lines were used, the dot was zeroed halfway between the right-hand ends of the two lines (see fig. 7). One of the four pilots preferred and used a single-reference-line display with the dot zeroed at its center. The two video signals were mixed for the final out-the-window display to the pilot. Since color television was used, the pilots were given a choice of red, blue, green, and white flare directors (i.e., lines and dot) superimposed on the airport scene. After trying each, they chose the white. The line(s)-dot display was also shifted with respect to the runway to allow the pilot to ascertain whether he preferred to monitor the flare director in his foveal, parafoveal, or peripheral vision. The pilots compromised on a location just to the left of the runway as shown in figure 7.
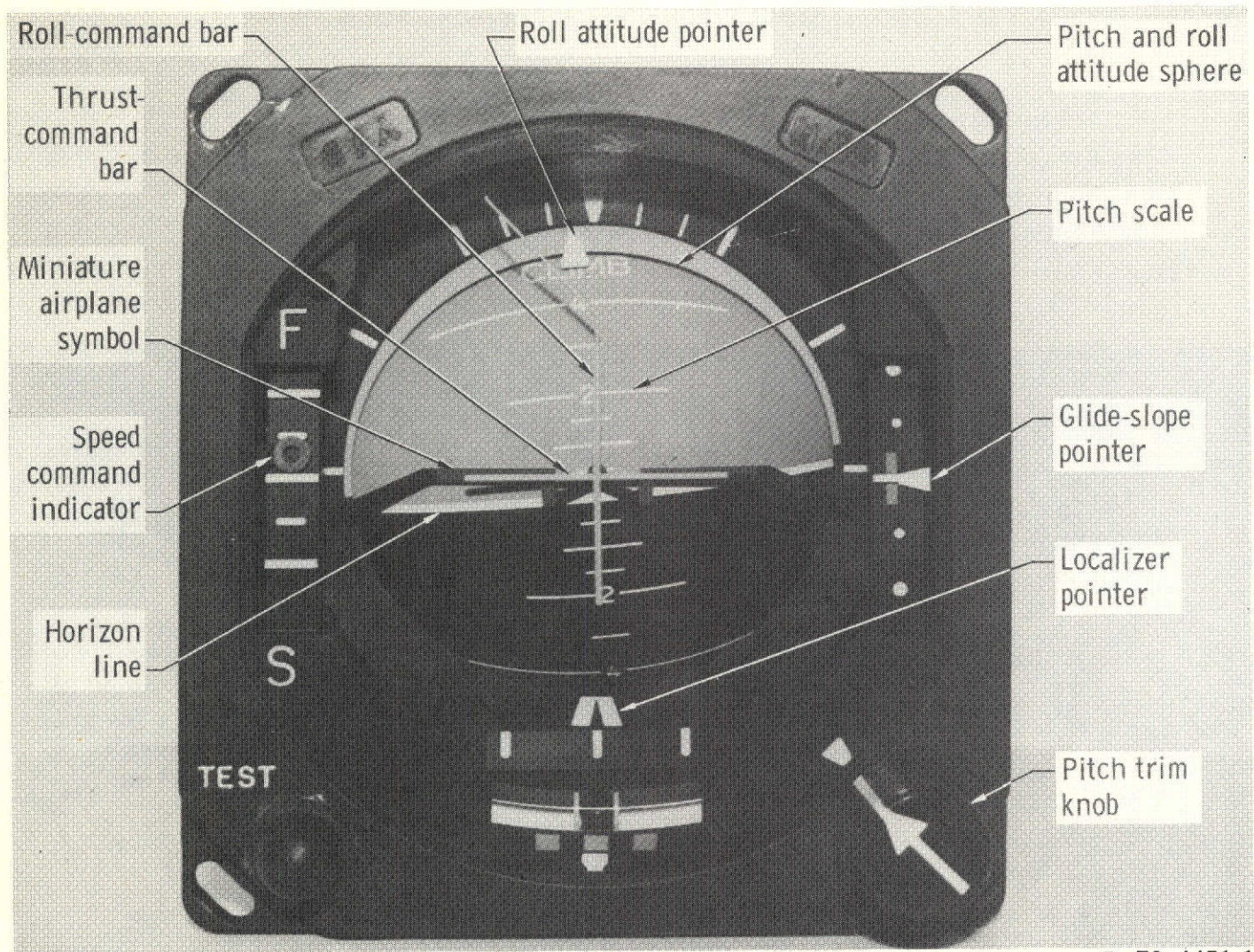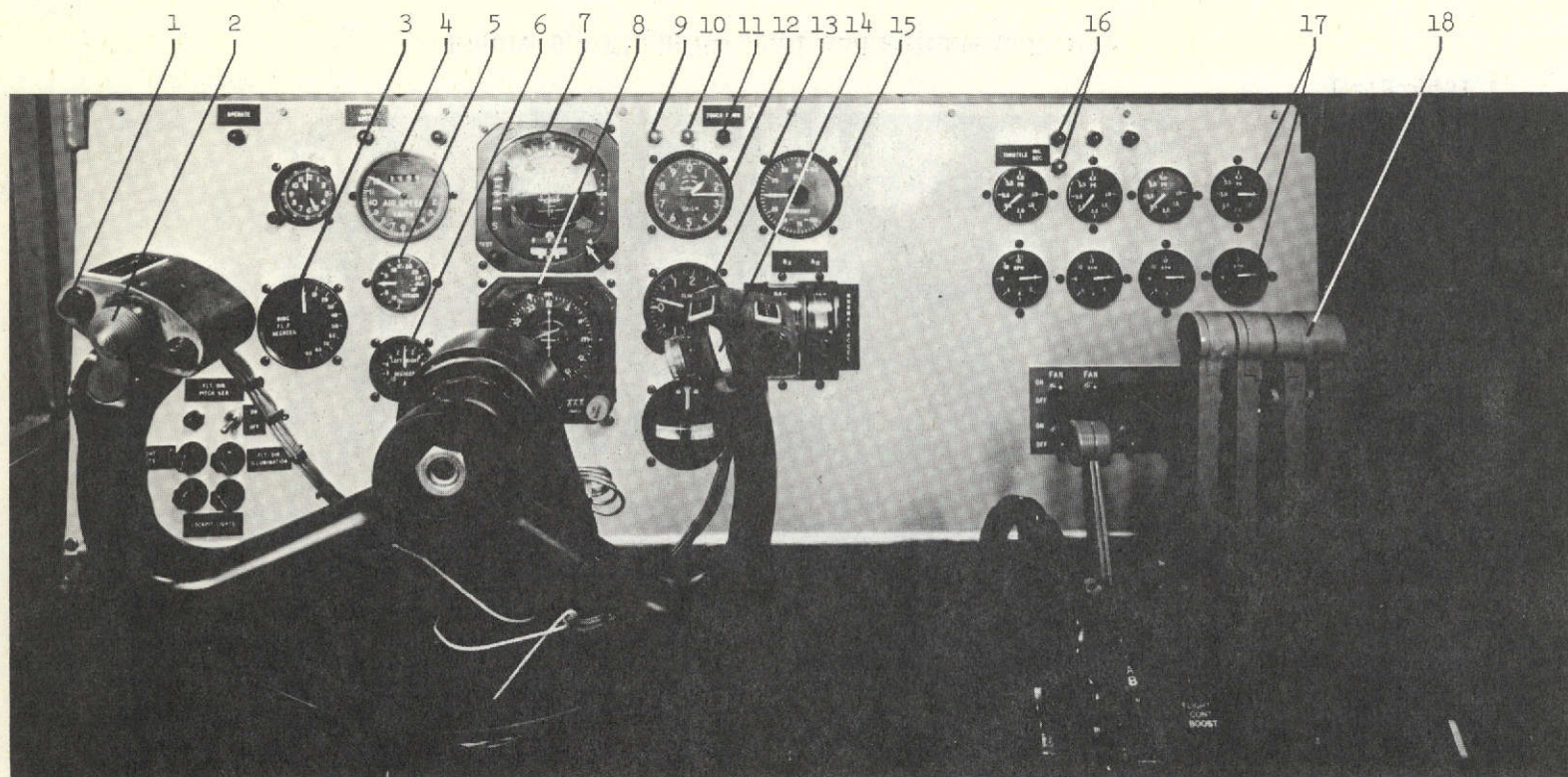
Figure 8.- Flight director and attitude indicator.

L-73-4451.1

1 Autospeed button
2 Pitch and roll trim
3 δ_{f3} flap
4 Airspeed
5 Angle of attack
6 Sideslip

7 Flight director
8 Horizontal situation indicator
9 Flare warning light
10 Flare initiation light
11 Touchdown light
12 Altimeter

13 Rate of climb
14 Direct-lift control wheel
15 Direct-lift control meter
16 Thrust trim lights
17 Engine instruments
18 Throttles

L-74-1151

Figure 9.- Pilot's view of cockpit interior.

Baseline groups C-1 and C-2 were made without the VFR flare director. In C-1, only the visual scene was used. Even though the average touchdown velocities $\dot{h}$ were fairly good, there was a wide scatter in the touchdown points and two obvious overflares. Without a definite guide for applying the flare thrust, the pilots tended to apply too much early in the maneuver and consequently drove the touchdown point beyond the landing zone. A primary complaint was that the television scene did not contain sufficient usable altitude and altitude-rate information. In subset C-2, a flare warning light was repositioned to the bottom of the windshield so that the pilot could see it come on as he looked out the window. The touchdown results were degraded. The pilots commented that a cue to help them start the flare at the proper time seemed like a good idea, but was of very little aid in helping them solve the basic problem of executing a correct thrust-flare program as a function of runway nearness, particularly when the television scene lacked good altitude-type cues. In subsets C-3 and C-4, the head-up flare-director display was added. Touchdown results were improved slightly in that the touchdown points were more concentrated and there were no overflares.

The pilots were strongly critical of nearly all aspects of the television display for the flare maneuver. In addition to the poor altitude cues, each pilot independently commented that he could not properly use the head-up flare director and still glean all of the important information from the "growing" airport scene. One pilot commented that he could use the head-up flare director as primary flare information and expect to make good landings, but that it was against all the principles of his training to be "viewing" an approaching runway scene without giving it his full attention. The other pilots concurred.

The VFR portion of the study was terminated when the pilots advised against a proposed short training program to determine whether they could learn to monitor the VFR flare director effectively in their parafoveal vision while concentrating on the runway. Their reasoning was that they felt they should not divide their attention in a critical situation such as landing. One pilot explained that several of his poorer VFR landings were due to changing his fixation momentarily from the director to the approaching runway scene and back. As a result, he gleaned information very poorly from both.

CONCLUDING REMARKS

A flare-director concept involving a "thrust-required" flare guidance equation has been developed and demonstrated during tests on a moving-base simulator. An externally blown flap STOL aircraft (with stability and control augmentation which included "autospeed" and "pitch-hold") was programed for the tests. Landing approaches were made at 75 knots along a 6° glide slope to a specified altitude where a constant-attitude power flare was initiated. A signal analogous to the flare equation was used to drive

head-up and instrument flare-director displays during a series of 28 simulated landings in both smooth air and moderate turbulence. For comparative purposes, the pilots made an additional 22 landings using the regular cockpit instruments or while looking out the window at the airport scene only. The 50 simulation runs produced the following findings:

1. Under instrument flight conditions, the flare director (presented on the horizontal command bar of the flight director) was considered a valuable guide in executing the proper thrust program during the relatively brief flares.

2. Under good visibility conditions, a head-up presentation of the flare director was rated undesirable because the pilots found it difficult to divide their attention between the visual scene and the superimposed flare director.

3. A 0.4-sec lead light during instrument landings helped the pilots apply the flare-initiation thrust-step promptly at the designated altitude and thus improved their touch-down values. The value of a similar light during the VFR runs was masked by the inherent deficiencies of a television display of the landing scene.

The pilots commented further that they could not fixate on the runway and effectively track the head-up flare director in their parafoveal vision, but that they could make good landings if they concentrated on the director. They said, however, that they felt very "uncomfortable" during this second situation because it was against the principles of their training to be looking in the vicinity of the runway and not giving it their foremost attention.

Langley Research Center,
National Aeronautics and Space Administration,
Hampton, Va., August 21, 1974.

REFERENCES

1. Grantham, William D.; Nguyen, Luat T.; Patton, James M., Jr.; Deal, Perry L.; Champine, Robert A.; and Carter, C. Robert: Fixed-Base Simulator Study of an Externally Blown Flap STOL Transport Airplane During Approach and Landing. NASA TN D-6898, 1972.

2. Miller, G. Kimball, Jr.; Deal, Perry L.; and Champine, Robert A.: Fixed-Base Simulation Study of Decoupled Controls During Approach and Landing of a STOL Transport Airplane. NASA TN D-7363, 1974.

3. Middleton, David B.; and Bergeron, Hugh P.: A Compilation and Analysis of Typical Approach and Landing Data for a Simulator Study of an Externally Blown Flap STOL Aircraft. NASA TN D-7497, 1974.

4. Parlett, Lysle P.; Greer, H. Douglas; Henderson, Robert L.; and Carter, C. Robert: Wind-Tunnel Investigation of an External-Flow Jet-Flap Transport Configuration Having Full-Span Triple-Slotted Flaps. NASA TN D-6391, 1971.

5. Grafton, Sue B.; Parlett, Lysle P.; and Smith, Charles C., Jr.: Dynamic Stability Derivatives of a Jet Transport Configuration With High Thrust-Weight Ratio and an Externally Blown Jet Flap. NASA TN D-6440, 1971.

6. Vogler, Raymond D.: Wind-Tunnel Investigation of a Four-Engine Externally Blowing Jet-Flap STOL Airplane Model. NASA TN D-7034, 1970.